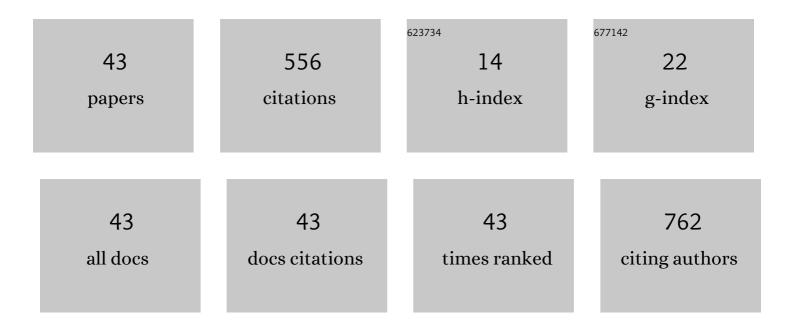
Wanjun Wang

List of Publications by Year in descending order

Source: https://exaly.com/author-pdf/3440957/publications.pdf Version: 2024-02-01



#	Article	IF	CITATIONS
1	Mode-locked operation characteristics of a monolithic integrated two-section InGaAs/GaAs double quantum wells laser with asymmetric waveguide. Optics and Laser Technology, 2022, 147, 107702.	4.6	1
2	Metal-insulator transition switching in <mml:math xmlns:mml="http://www.w3.org/1998/Math/MathML"><mml:msub><mml:mrow><mml:mi>VO</mml:mi>heterojunctions. Physical Review Materials, 2022, 6, .</mml:mrow></mml:msub></mml:math 	:mt20x4V> <m< td=""><td>וml:mi>x</td></m<>	וm l :mi>x
3	Strain engineering for pseudo-magnetic fields in graphene. , 2022, , .		0
4	Modal gain characteristics of a two-section InGaAs/GaAs double quantum well passively mode-locked laser with asymmetric waveguide. Scientific Reports, 2022, 12, 5010.	3.3	1
5	Wafer-Scale Demonstration of Low-Loss (â^1⁄40.43 dB/cm), High-Bandwidth (>38 GHz), Silicon Photonics Platform Operating at the C-Band. IEEE Photonics Journal, 2022, 14, 1-9.	2.0	8
6	Ligand size effects in two-dimensional hybrid copper halide perovskites crystals. Communications Materials, 2021, 2, .	6.9	12
7	Hole selective WOx and V2Ox contacts using solution process for silicon solar cells application. Materials Chemistry and Physics, 2021, 273, 125101.	4.0	11
8	Stable Mode-Locked Operation With High Temperature Characteristics of a Two-Section InGaAs/GaAs Double Quantum Wells Laser. IEEE Access, 2021, 9, 16608-16614.	4.2	1
9	Compact, Hybrid III-V/Silicon Vernier Laser Diode Operating From 1955–1992 nm. IEEE Photonics Journal, 2021, 13, 1-5.	2.0	1
10	Temperature-dependent phase noise properties of a two-section GaSb-based mode-locked laser emitting at 21¼m. Applied Physics Letters, 2020, 117, 141103.	3.3	2
11	Analysis of Compact Silicon Photonic Hybrid Ring External Cavity (SHREC) Wavelength-Tunable Laser Diodes Operating From 1881–1947 nm. IEEE Journal of Quantum Electronics, 2020, 56, 1-11.	1.9	4
12	1 × N (N = 2, 8) Silicon Selector Switch for Prospective Technologies at the 2 μm Waveband. IEEE Photonics Technology Letters, 2020, 32, 1127-1130.	2.5	12
13	Carrier selective solution processed molybdenum oxide silicon heterojunctions solar cells with over 12% efficiency. Semiconductor Science and Technology, 2020, 35, 075022.	2.0	13

14	Wafer-Level Characterization of Silicon Nitride CWDM (De)Multiplexers Using Bayesian Inference. IEEE Photonics Technology Letters, 2020, 32, 917-920.	2.5	5
15	Compact silicon photonic hybrid ring external cavity (SHREC)/InGaSb-AlGaAsSb wavelength-tunable laser diode operating from 1881-1947â€nm. Optics Express, 2020, 28, 5134.	3.4	17
16	Sub-kHz linewidth, hybrid III-V/silicon wavelength-tunable laser diode operating at the application-rich 1647-1690â€nm. Optics Express, 2020, 28, 25215.	3.4	14

17	High temperature characteristics of a 2 <i>μ</i> m InGaSb/AlGaAsSb passively mode-locked quantum well laser. Applied Physics Letters, 2019, 114, .	3.3	8	
	Mid-Infrared, Ultra-Broadband, Low-Loss, Compact Arbitrary Power Splitter Based on Adiabatic Mode			

18Mid-Infrared, Ultra-Broadband, Low-Loss, Compact Arbitrary Power Splitter Based on Adiabatic Mode2.01818Evolution. IEEE Photonics Journal, 2019, 11, 1-11.2.018

WANJUN WANG

#	Article	IF	CITATIONS
19	High-performance 1.06- <i>μ</i> m InGaAs/GaAs double-quantum-well semiconductor lasers with asymmetric heterostructure layers. Semiconductor Science and Technology, 2019, 34, 055013.	2.0	9
20	SiN-SOI Multilayer Platform for Prospective Applications at 2 μm. IEEE Photonics Journal, 2019, 11, 1-9.	2.0	3
21	Extracting more light for vertical emission: high power continuous wave operation of 1.3-μm quantum-dot photonic-crystal surface-emitting laser based on a flat band. Light: Science and Applications, 2019, 8, 108.	16.6	22
22	Integrating GeSn photodiode on a 200 mm Ge-on-insulator photonics platform with Ge CMOS devices for advanced OEIC operating at 2 μm band. Optics Express, 2019, 27, 26924.	3.4	28
23	Wavelength-Flattened Directional Coupler Based Mid-Infrared Chemical Sensor Using Bragg Wavelength in Subwavelength Grating Structure. Nanomaterials, 2018, 8, 893.	4.1	42
24	Experimental Demonstration of Thermally Tunable Fano and EIT Resonances in Coupled Resonant System on SOI Platform. IEEE Photonics Journal, 2018, 10, 1-8.	2.0	6
25	Spiral Waveguides on Germanium-on-Silicon Nitride Platform for Mid-IR Sensing Applications. IEEE Photonics Journal, 2018, 10, 1-7.	2.0	23
26	Investigation of regime switching from mode locking to Q-switching in a 2 Âμm InGaSb/AlGaAsSb quantum well laser. Optics Express, 2018, 26, 8289.	3.4	13
27	Monolithic Fabrication of InGaAs/GaAs/AlGaAs Multiple Wavelength Quantum Well Laser Diodes via Impurity-Free Vacancy Disordering Quantum Well Intermixing. IEEE Journal of the Electron Devices Society, 2017, 5, 122-127.	2.1	5
28	Temperature- and current-dependent spontaneous emission study on 2 µm InGaSb/AlGaAsSb quantum well lasers. Japanese Journal of Applied Physics, 2017, 56, 050310.	1.5	4
29	High-Speed and High-Responsivity InP-Based Uni-Traveling-Carrier Photodiodes. IEEE Journal of the Electron Devices Society, 2017, 5, 40-44.	2.1	4
30	Surface Plasmon Enhanced Nitrogenâ€Doped Graphene Quantum Dot Emission by Single Bismuth Telluride Nanoplates. Advanced Optical Materials, 2017, 5, 1700176.	7.3	18
31	Low-threshold optically pumped lasing in highly strained germanium nanowires. Nature Communications, 2017, 8, 1845.	12.8	131
32	Modal gain characteristics of a 2 <i>μ</i> m InGaSb/AlGaAsSb passively mode-locked quantum well laser. Applied Physics Letters, 2017, 111, .	3.3	20
33	Electromagnetically induced transparency-like effect in microring-Bragg gratings based coupling resonant system. Optics Express, 2016, 24, 25665.	3.4	20
34	On-Chip Air-Gapped Cavity Resonators and Filters for mm-Wave IC Applications. IEEE Transactions on Components, Packaging and Manufacturing Technology, 2016, 6, 1549-1554.	2.5	4
35	Characterization of highâ€photocurrent and highâ€speed INPâ€based uniâ€travelingâ€carrier photodiodes at 1.55â€Ĥ4m wavelength. Microwave and Optical Technology Letters, 2016, 58, 2156-2162.	1.4	2
36	A compact ultrabroadband polarization beam splitter utilizing a hybrid plasmonic Y-branch. IEEE Photonics Journal, 2016, , 1-1.	2.0	16

Wanjun Wang

#	Article	IF	CITATIONS
37	Low-Loss Microcoaxial Rat-Race Hybrid for Si-Based Microwave Integrated Circuits. IEEE Microwave and Wireless Components Letters, 2016, 26, 162-164.	3.2	4
38	A Polarization Splitter and Rotator Based on a Partially Etched Grating-Assisted Coupler. IEEE Photonics Technology Letters, 2016, 28, 911-914.	2.5	15
39	Low-Loss Microcoax-to-CPW Transition for Air-gapped Microcoaxial Passives. IEEE Microwave and Wireless Components Letters, 2015, 25, 585-587.	3.2	6
40	Airâ€gapped microcoxial transmission line for ultrawide band microwave and millimeter wave ICS. Microwave and Optical Technology Letters, 2014, 56, 1462-1465.	1.4	7
41	High-Photocurrent and Wide-Bandwidth UTC Photodiodes With Dipole-Doped Structure. IEEE Photonics Technology Letters, 2014, 26, 1952-1955.	2.5	5
42	A 390 ps On-Wafer True-Time-Delay Line Developed by a Novel Micro-Coax Technology. IEEE Microwave and Wireless Components Letters, 2014, 24, 233-235.	3.2	18
43	An enhanced charge carrier separation in a heterojunction solar cell with a metal oxide. Physica Status Solidi (A) Applications and Materials Science, 0, , 2100525.	1.8	2